

## Structural investigations of epitaxial InN by x-ray photoelectron diffraction and x-ray diffraction

Daniel Hofstetter,<sup>a)</sup> Laurent Despont, M. Gunnar Garnier, Esther Baumann, Fabrizio R. Giorgetta, and Philipp Aebi

*Institute of Physics, University of Neuchatel, 1 A.-L. Breguet, CH-2000 Neuchatel, Switzerland*

Lutz Kirste

*Fraunhofer Institute of Applied Solid State Physics, Tullastrasse 72, D-79108 Freiburg, Germany*

Hai Lu<sup>b)</sup> and William J. Schaff

*ECE Department, Cornell University, Phillips Hall 425, Ithaca, New York 14853*

The authors investigated a 1  $\mu\text{m}$  thick molecular beam epitaxy-grown InN film by means of full hemispherical x-ray photoelectron diffraction and high resolution x-ray diffraction. While x-ray diffraction reveals that this nominally hexagonal InN layer contains roughly 1% of cubic phase InN, a comparison between measured and simulated x-ray photoelectron diffraction data allowed them to directly determine the polarity of the crystal. Furthermore, the data indicate that the InN surface consists of a mosaic of domains oriented at an azimuth of  $180^\circ$  to each other, where the azimuth corresponds to the rotation angle around the [0001] axis.

During the past 15 years, the III-nitrides have experienced a very intense period of research. Main triggers for this development were InGaN/GaN-based violet light emitters for optical data storage and white light generation, and also AlGaIn-based high electron mobility transistors for high power density electronics.<sup>1,2</sup> However, since the III-nitride research was mainly application driven, several issues of fundamental importance did not receive their due attention and thus remained unsolved for a surprisingly long time. As the most striking example, InN was believed to have a band gap energy of 1.89 eV since 1977.<sup>3</sup> Mostly thanks to improved growth methods, high quality InN films became available in 2001, and in 2002, the true room temperature band gap energy of InN, namely, 0.62 eV, was discovered.<sup>4,5</sup> During the following years, the available high quality InN films revealed further surprising properties. As an example, the relative positions of the pinned Fermi level and the conduction band minimum in InN lead to a huge surface electron accumulation; this is in contrast to GaN and AlN which exhibit an electron depletion.<sup>6</sup> For applications such as laser diodes and transistors, other parameters such as surface roughness, dislocation density, and polarity of the material are of crucial importance. Laser cavities, for instance, must have low losses in order to yield devices with a reasonably small threshold current density. Unfortunately, both columnar growth mode and stacking faults typical for III-nitride epitaxy on sapphire lead to dislocations, which inevitably result in cavity losses. The understanding of domain formation in InN and their mutual orientation are therefore topics which have an interest reaching beyond pure material science.<sup>7</sup> As a last example, the functioning of a III-nitride based transistor requires a two dimensional electron gas close to the crystal surface, which will occur only if the correct material polarity is used. Many different methods

for polarity determination have been reported for the III-nitrides.<sup>8,9</sup> On InN samples, convergent beam electron diffraction is the only nondestructive method used so far.<sup>10</sup> X-ray photoelectron diffraction (XPD), which is nondestructive as well, has been employed for investigations of tetragonality,<sup>11</sup> surface polarity,<sup>12</sup> and crystal orientation in various materials, including GaN.<sup>9,13</sup> Here, we use this versatile technique to determine the polarity of a 1  $\mu\text{m}$  thick, high quality InN film, and to gain information about domain formation on its surface.

Fabrication of the InN film was accomplished by plasma-assisted molecular beam epitaxy. The structure is grown on C-face sapphire substrates and contains a 50 nm thick AlN nucleation layer, followed by roughly 250 nm of GaN. Between this buffer and the subsequent 1  $\mu\text{m}$  thick InN layer, a six period InN/InGaIn superlattice with a nominal period of 15 nm was inserted. The purpose of this stack was to bend dislocations and to improve the subsequently grown InN material quality. Although group V—face nitrides can be fabricated, the growth conditions chosen for the AlN nucleation and the GaN buffer layers usually result in group III—face of the deposited material. Prior to the XPD measurements, the InN surface was cleaned *in situ* using soft oxygen plasma.

XPD measurements are performed at room temperature in a modified Vacuum Generators ESCALAB Mark II x-ray photoelectron spectrometer equipped with a fixed hemispherical electron energy analyzer, a three channeltron detection system, an x-ray photon source [ $h\nu=1253.6\text{ eV}$  (Mg  $K\alpha$ )], and a computer-controlled two-axis goniometer. This setup is capable of scanning the electron collection angle over the full hemisphere above the surface<sup>14</sup> and operates with a base pressure in the lower  $10^{-11}$  mbar region. The data have been collected for a polar angle range  $\theta \in (0^\circ, 70^\circ)$  and an azimuthal angle range  $\phi \in (0^\circ, 360^\circ)$ . As described in more detail in Ref. 14, XPD probes the local geometry around a selected atom by performing an intensity

<sup>a)</sup>Electronic mail: daniel.hofstetter@unine.ch

<sup>b)</sup>Present address: Department of Physics, Nanjing University, Nanjing 210093, China.

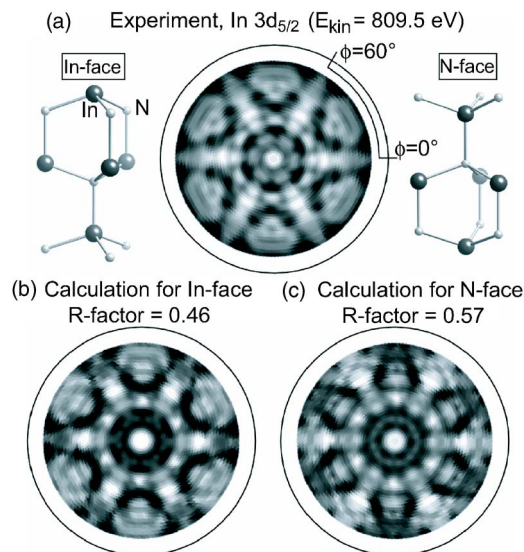


FIG. 1. (Color online) Stereographic projections of measured (a) and two-fold symmetrized single-scattering simulated diffractograms for In- (b) and N-face (c) configurations using In  $3d_{5/2}$  photoelectrons at 809.5 eV ( $Mg K\alpha$ ). The better agreement between experiment (a) and simulated In-face configuration (b) is obvious.

versus emission-angle scan of a particular photoemission line. Since the line energy is specific for the core levels of the selected atom type, XPD is chemically sensitive. The outgoing photoemitted electrons exhibit a strongly anisotropic angular intensity distribution, which is due to the interference of the directly emitted photoelectron wave with the scattered electron waves. When considering a row of atoms, scattering at the first few atoms along this row focuses the electron flux in the emitter-scatterer direction (forward focusing). The method is thus also capable to reveal structural information of the sample surface.

In order to better understand the collected data, single-scattering calculations have been performed to simulate the experimental diffractograms.<sup>15</sup> No structure optimization has been made to simulate the XPD pattern; instead, literature InN lattice parameters have been employed ( $a=b=0.3544$  nm and  $c=0.5718$  nm) (Ref. 16) to create a cluster containing 1211 atoms. For the selected In  $3d_{5/2}$  photoelectron kinetic energy ( $E_{kin}=809.5$  eV), a photoelectron inelastic mean free path of 0.8 nm was used with five In emitters down to a depth of approximately 1.2 nm below the surface.

To obtain a quantitative value of the agreement between calculated and measured diffractograms, a reliability factor ( $R_{factor}$ ) analysis based on the multipole expansion of the angular intensity distribution, i.e., the expansion into spherical harmonics, has been used.<sup>17</sup> Measured and calculated diffractograms of InN (0001)  $3d_{5/2}$  are presented in Fig. 1 using the same linear gray scale and stereographic projection. According to the InN crystal structure, a threefold symmetrization for improving the measurement contrast has been applied to the experimental diffractogram. However, even without performing this symmetrization procedure, the obtained result is sixfold symmetric, quite in contrast to the predicted threefold symmetry. This observation made by the eyes is confirmed by a global match approach using the aforementioned  $R_{factor}$ . For both In-face and N-face materials, the additional  $180^\circ$  symmetry improves the agreement. A considerably better agreement between experiment and

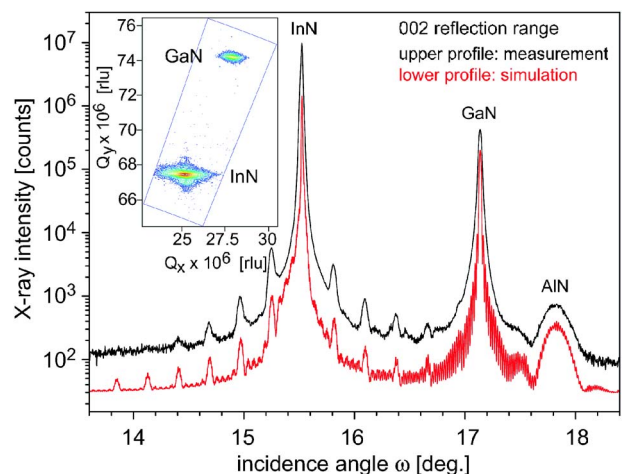


FIG. 2. (Color online) HRXRD  $\omega$ - $2\theta$  scan of the (002) reflection range. The superlattice period deduced here was  $16.2 \pm 0.1$  nm. The inset shows a HRXRD reciprocal space map measured around the (105) reflection.

single-scattering calculation is obtained for the  $180^\circ$  symmetrized In face ( $R_{factor}=0.46$ ) than for the N-face configuration ( $R_{factor}=0.57$ ). In contrast, the difference between In or N termination is not significant. At this point, we would like to stress that XPD allows a nondestructive determination of the material polarity. In addition, our findings confirm earlier results on a similar sample obtained by ion scattering spectroscopy.<sup>18</sup> A legitimate question concerns the reason for the experimental sixfold symmetry of the XPD pattern. The expected threefold symmetry of the diffractogram would be observed only on a perfectly flat single-crystal surface. Since InN grows typically with a surface roughness of more than 1 ML and in terraces, this requirement is certainly not fulfilled. Furthermore, columnar growth and stacking faults within the film lead to entire domains which are rotated around the  $[0001]$  axis by  $180^\circ$  with respect to each other. All of the above effects together can easily explain the observed sixfold symmetry of the XPD pattern.

To gain further insight into the material properties, high resolution x-ray diffraction (HRXRD)  $\omega$ - $2\theta$  scans, rocking curve measurements, and reciprocal space mappings were performed. For these measurements, a Panalytical materials research diffractometer equipped with a hybrid two-bounce Ge-220 monochromator and a triple axis Ge-220 analyzer was employed. For extended bond measurements, we used a high resolution diffractometer setup with a four-bounce Ge-220 monochromator (Bartels-DuMond type) with open ended detector, whereas XRD texture measurements were performed with a focusing x-ray diffractometer with a bended Ge-111 monochromator. The details of the various x-ray diffractometry setups are described elsewhere.<sup>19</sup> Figure 2 shows a HRXRD  $\omega$ - $2\theta$  scan around the (002) reflection of the investigated InN crystal. From the angular separation and the intensity of the superlattice satellite peaks, we estimated by profile simulations a period of  $16.2 \pm 0.1$  nm and single layer thicknesses of  $15.8 \pm 0.2$  nm InN and  $0.4 \pm 0.2$  nm,  $In_{0.5}Ga_{0.5}N$ , respectively. The texture diffractometry azimuthal scan of the (101) reflection shown in Fig. 3 (top) confirms the hexagonal symmetry of the InN wurtzite-type structure. In addition, a negligibly small (roughly 1%) amount of cubic phase InN with sphalerite-type structure could be detected by measuring an azimuthal scan of the cubic InN (200) reflection, as shown in Fig. 3 (bottom). Such

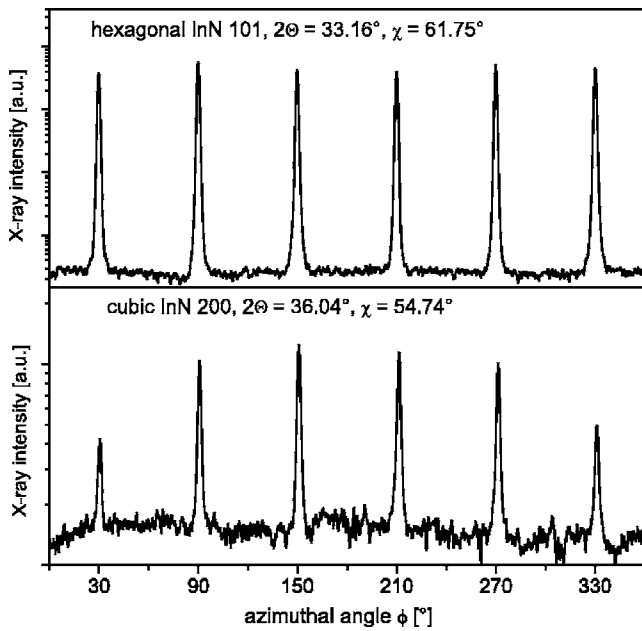


FIG. 3. (Top) Azimuthal scan around the (101) reflection of InN at a polar angle of  $61.75^\circ$ . A sixfold symmetry was observed. (Bottom) Azimuthal scan around the (200) reflection of InN at a polar angle of  $54.74^\circ$ . This measurement confirms the existence of roughly 1% of cubic phase InN.

a small amount of cubic phase indicates occasional vertical stacking faults in the film. This is consistent with the existence of InN columns whose lower part is hexagonally close packed in *ABAB* stacking, whereas their upper part exhibits *ACAC* stacking. At the interface of the two stackings, cubic material with a stacking order *ABABABCACAC* (face-centered-cubic stacking underlined) occurs.

Extended bond measurements using the InN (006) and (105) reflections and reciprocal space maps of the InN (002) and (105) reflections (inset of Fig. 2) were applied to determine the InN lattice parameters.<sup>19</sup> Both measurement techniques showed a close agreement resulting in lattice parameters of  $a=0.353\,34\pm 0.000\,04$  nm and  $c=0.571\,35\pm 0.000\,02$  nm, leading to a  $c/a$  ratio of  $1.6170\pm 0.0002$ . The estimated lattice parameters of the InN indicate that a compressive biaxial strain within the layer is present. This strain is due to a mismatch in both the thermal expansion coefficients and the in-plane lattice parameters of the InN layer and the GaN buffer. Using elastic parameters from the literature,<sup>20</sup> the unstrained metric of the InN layer was evaluated to  $a=0.353\,96\pm 0.000\,02$  nm and  $c=0.570\,53\pm 0.000\,03$  nm, leading to a  $c/a$  ratio of  $1.6118\pm 0.0002$ . These values are in good agreement with recent literature values measured on similar InN samples.

In order to examine the defect structure of the InN layer, GAUSSIAN fits to the rocking curves of the (002), (004), and (006) reflections were performed. Then a procedure similar to a Williamson-Hall analysis yielded a mean lateral column size of 246 nm and a tilt of  $0.31^\circ$ . Given the small lateral size of the columns and the inherent averaging of the XPD mea-

surement over a relatively large surface of  $5\times 5$  mm<sup>2</sup>, it is obvious that even in a perfectly flat crystal the orientation of a single columnar crystallite could not show up in XPD.

In conclusion, we have shown detailed XPD and HRXRD analyses of bulk InN grown by molecular beam epitaxy. A comparison between measured and calculated XPD diffraction pattern shows an In face of the InN film. In contrast to the simulation, our experiment reveals a sixfold symmetry of the XPD pattern. It indicates that the surface of InN grown on a GaN buffer is a mosaic of domains with two  $180^\circ$  different azimuthal orientations around the [0001] axis.

The authors would like to thank the U.S. Office of Naval Research and the Professorship Program and the National Center of Competence in Research MaNEP, both from the Swiss National Science Foundation for their generous financial support.

<sup>1</sup>S. Nakamura and G. Fasol, *The Blue Laser Diode* (Springer, Heidelberg, 1997)

<sup>2</sup>O. Ambacher, J. Majewski, C. Miskys, A. Link, M. Hermann, M. Eickhoff, M. Stutzmann, F. Bernardini, V. Fiorentini, V. Tilak, B. Schaff, and L. F. Eastman, *J. Phys.: Condens. Matter* **14**, 3399 (2002).

<sup>3</sup>V. A. Tygai, A. M. Evstigneev, A. N. Krasiko, A. F. Andreeva, and V. Y. Malakhov, *Sov. Phys. Semicond.* **11**, 1257 (1977).

<sup>4</sup>V. Yu. Davydov, A. A. Klochikhin, R. P. Seisyan, V. V. Emtsev, S. V. Ivanov, F. Bechstedt, J. Furthmüller, H. Harima, A. V. Mudryi, J. Aderhold, O. Semchinova, and J. Graul, *Phys. Status Solidi B* **229**, R1 (2002).

<sup>5</sup>J. Wu, W. Walukiewicz, K. M. Yu, J. W. Ager III, E. E. Haller, H. Lu, W. J. Schaff, Y. Saito, and Y. Nanishi, *Appl. Phys. Lett.* **80**, 3967 (2001).

<sup>6</sup>T. D. Veal, P. H. Jefferson, L. F. J. Piper, C. F. McConville, T. B. Joyce, P. R. Chalker, L. Considine, H. Lu, and W. J. Schaff, *Appl. Phys. Lett.* **89**, 202110 (2006).

<sup>7</sup>E. Valcheva, T. Paskova, P. O. A. Persson, L. Hultman, and B. Monemar, *Appl. Phys. Lett.* **80**, 1550 (2002).

<sup>8</sup>A. Kazimirov, G. Scherb, J. Zegenhagen, T.-L. Lee, M. J. Bedzyk, M. K. Kelly, H. Angerer, and O. Ambacher, *J. Appl. Phys.* **84**, 1703 (1998), and references therein.

<sup>9</sup>J. L. Rouviere, J. L. Weyher, M. Seilmann-Eggebert, and S. Porowski, *Appl. Phys. Lett.* **73**, 668 (1998).

<sup>10</sup>T. Mitate, S. Mizuno, H. Takahata, R. Kakegawa, T. Matsuoka, and N. Kuwano, *Appl. Phys. Lett.* **86**, 134103 (2005).

<sup>11</sup>L. Despont, C. Koitzsch, F. Clerc, M. G. Garnier, P. Aebi, C. Lichtensteiger, J.-M. Triscone, F. J. Garcia de Abajo, E. Bousquet, and Ph. Ghosez, *Phys. Rev. B* **73**, 094110 (2006).

<sup>12</sup>L. Despont, F. Clerc, M. G. Garnier, H. Berger, L. Forró, and P. Aebi, *Eur. Phys. J. B* **52**, 421 (2006).

<sup>13</sup>M. Seilmann-Eggebert, J. L. Weyher, H. Obloh, H. Zimmermann, A. Rar, and S. Porowski, *Appl. Phys. Lett.* **71**, 2635 (1997).

<sup>14</sup>J. Osterwalder, T. Greber, A. Stuck, and L. Schlappbach, *Phys. Rev. B* **44**, 13764 (1991).

<sup>15</sup>C. S. Fadley, *Synchrotron Radiation Research: Advances in Surface Science* (Plenum, New York, 1990).

<sup>16</sup>S. Strite and H. Morkoc, *J. Vac. Sci. Technol. B* **10**, 1237 (1992), and references therein.

<sup>17</sup>R. Fasel, P. Aebi, J. Osterwalder, L. Schlappbach, R. G. Agostino, and G. Chiarello, *Phys. Rev. B* **50**, 14516 (1994).

<sup>18</sup>M. Walker, T. D. Veal, H. Lu, W. J. Schaff, and C. F. McConville, *Phys. Status Solidi C* **2**, 2301 (2005).

<sup>19</sup>N. Herres, L. Kirste, H. Obloh, K. Köhler, J. Wagner, and P. Koidl, *Mater. Sci. Eng., B* **91-92**, 425 (2002).

<sup>20</sup>A. F. Wright, *J. Appl. Phys.* **82**, 2833 (1997).